American Journal of Modern Physics
2015; 4(1-1): 23-29
Published online December 26, 2014 (http://www.sciencepublishinggroup.com/j/ajmp)
doi: 10.11648/j.ajmp.s.2015040101.15
ISSN: 2326-8867 (Print); ISSN: 2326-8891 (Online)

Development of a new type of germanium detector for dark matter searches

Wenzhao Wei[1], Hao Mei[1], GuojianWang[1], Gang Yang[1], Chao Zhang[1], Yutong Guan[1], Jing Liu[1], Dongming Mei[1, 2, *], Christina Keller[1], Yiju Wang[2], Dahai Xu[2]

[1]Department of Physics, The University of South Dakota, Vermillion, SD 57069, United States
[2]School of Physics and Optoelectronic, Yangtze University, Jingzhou 434023, China

Email address:

Wenzhao.Wei@usd.edu (Wenzhao Wei), Hao.Mei@usd.edu (Hao Mei), Guojian.Wang@usd.edu (Guojian Wang), Gang.Yang@usd.edu (Gang Yang), Chao.Zhang@usd.edu (Chao Zhang), Yutong.Guan@usd.edu (Yutong Guan), Jing.Liu@usd.edu (Jing Liu), Dongming.Mei@usd.edu (Dongming Mei), Tina. Keller@usd.edu (Christina Keller), wang@yangtzeu.edu.cn (Yiju Wang), dhxu@yangtzeu.edu.cn (Dahai Xu)

To cite this article:

Wenzhao Wei, Hao Mei, GuojianWang, Gang Yang, Chao Zhang, Yutong Guan, Jing Liu, Dongming Mei, Christina Keller, Yiju Wang, Dahai Xu. Development of a New Type of Germanium Detector for Dark Matter Searches. *American Journal of Modern Physics*. Special Issue: New Science Light Path on Cosmological Dark Matters. Vol. 4, No. 1-1, 2015, pp. 23-29. doi: 10.11648/j.ajmp.s.2015040101.15

Abstract: A new type of germanium (Ge) detector for dark matter searches is under development utilizing the Ge crystal growth facility recently established at the University of South Dakota. Detector-grade crystals with electric impurity levels within $10^{10}/cm^3$ and neutral impurity levels within $10^{14}/cm^3$ have been grown regularly in the laboratory. These crystals can be fabricated into planar detectors with 1cm in thickness and 10cm in diameter. When a high voltage is applied to one of the end planes, a uniform electric field in the volume can be established. Such a design could result in a very fast electric signal. A time resolution of 1ns is expected by combining a short drift length and large drift mobility. This may allow us to resolve the difference on the electric pulse rise-time between low-energy nuclear recoil events and electronic recoil events at liquid nitrogen temperatures. An array of 168 planar detectors of this kind was modeled in a Geant4-based Monte Carlo simulation package. Its background reduction power was investigated and its sensitivity in dark matter search is estimated to be ~$10^{-48}cm^2$.

Keywords: Nuclear Recoil, Rise Time Difference, Crystal Growth, Dark Matter Searches

1. Introduction

Various astronomical observations provide strong evidence for the existence of dark matter in the universe [1-3]. The so-called Weakly Interacting Massive Particles (WIMPs) are among the most plausible candidates [4-15]. They can be detected directly through observations of nuclear recoils (NR) produced when they scatter with nuclei of the target material of a detector located in a deep underground laboratory in which cosmic ray induced backgrounds are strongly suppressed by the overlaying rocks and by proper shielding. However, natural radiation from a detector and its surrounding materials may introduce electronic recoil (ER) events in the detector. These ER events are orders of magnitude higher than dark matter induced NR events. The Cryogenic Dark Matter Search (CDMS) experiment operates germanium and silicon bolometers at ~50mK [7, 10, 12]. The NR events can be distinguished from ER events by their difference in the ratio of ionization signals and phonon signals. However, the required low temperature operation makes it expensive to adopt such a technique in the next generation of ton-scale dark matter experiments. The CoGeNT [11] experiment uses p-type point-contact (PPC) germanium detectors to search for dark matter. They operate at liquid nitrogen temperatures, which make it relatively easier and economical to build a ton-scale experiment using this technique. Unfortunately, PPC Ge detectors cannot provide NR/ER discrimination. A new-type of detector that provides NR/ER discrimination at liquid nitrogen temperatures would overcome disadvantages faced by CDMS and CoGeNT and, with an effective threshold lower than 100eV, open up fresh opportunities for the direct detection of dark matter at ton-scale, measurements of the neutrino magnetic moment and neutrino-nucleus coherent scattering, and detection of solar pp-neutrinos [16].

Such a detector can be realized if its time resolution is

good enough that it can resolve the difference of the rise time of electronic signals induced by NR and ER events. The rise time is primarily determined by the drift velocities of charge carriers and the geometry of the germanium crystal. The rise time from a typical PPC and coaxial Ge detectors are of the order of ~1μs and ~100ns, respectively. It can be shortened by: 1) a detector-grade crystal grown with electronic impurity levels within 10^{10}/cm^3 uniformly distributed across the entire crystal; 2) a detector fabricated in a planar shape with uniform electric field lines; and 3) amorphous-germanium contacts to eliminate a transition layer which causes slow pulses.

In this work, the capability to grow Ge crystals with sufficiently low impurity level at The University of South Dakota (USD) is described in Section 2. The Monte Carlo simulation of an array of the new type of Ge detectors is presented in Section 3. The background rejection power of this array is studied based on simulation and is presented in Section 4. In section 5, we conclude that the proposed Ge detector array has great potential to be used in the next generation of Ge-based ton-scale experiments for dark matter detection.

2. USD Capability for Ge Crystal Growth

USD has established a Ge crystal growth facility, which includes zone refinement, crystal growth and characterization, and detector development [17-23]. Mark Amman at Lawrence Berkeley National Laboratory (LBNL) and Yulan Li at Tsinghua University have successfully fabricated Ge detectors with the crystals from USD [24]. The infrastructure at USD, focused on crystal growth, is the first of its kind in the world for a research institution. The existing specific research capabilities include the ability to: 1) purify commercially available germanium ingots down to ~10^{10}/cm^3 using zone refinement techniques; 2) grow detector-grade germanium single crystals with large diameters (up to 10cm) and low-dislocation densities (10^2-10^4/cm^3) using the Czochralski method (which preserves the impurity level of 10^{10}/cm^3 obtained by zone refinement); 3) characterize the grown crystals using appropriate tools and methods; and 4) fabricate detectors from the grown crystals in order to verify that they are detector grade.

2.1. Zone Refinement

In the process of preparing high-purity germanium (HPGe) single crystals for fabrication into detectors, zone refinement is one of the very important procedures to purify germanium ingots used for growing crystals in our laboratory. In zone refinement of high-purity germanium crystals, the influential factors include cleaning procedures for raw materials, quartz tubes and containers for raw materials, vacuum level, container types, ambient gases, speed of zone travel, the ratio of ingot length to molten zone length, etc. In the present work, we have investigated the influences of cleaning procedures, boats for holding germanium ingots, vacuum levels of the chamber, and speed of zone travel and the ratio of ingot length to molten zone length [23]. There are two units of zone refiners with a total capacity of 20-kg per two weeks in the zone refinement laboratory.

2.2. Crystal Growth

Ton-scale HPGe crystals are needed for dark matter and neutrino experiments. HPGe crystals grown in a surface environment will be contaminated by cosmic rays. In collaborating with the Sanford Underground Research Facility (SURF), we explore HPGe crystal growing and fabrication processes underground. Two crystal growers were installed at the Advanced Materials for Underground Physics (AMUP) laboratory at USD for crystal growth (Fig. 1, Right). The crystals grown with these two growers have diameters as large as 10cm. A water chiller provides cooling for crystal growth.

HPGe crystals are grown using the Czochralski method and in highly pure hydrogen atmosphere (Fig. 1, Left). Growing detector-grade germanium crystals is very demanding and highly challenging as established by pioneer Eugene Haller and his colleagues at LBNL [25-31]. A detailed protocol is required for converting bulk germanium into ultra-pure material used in detectors of rare event physics experiments. The net impurity concentration and the dislocation density of the grown crystals have only a narrow range of values that are acceptable for large-volume coaxial or point contact germanium detector fabrication. They must be in the range of 0.5 – 3.0×10^{10}/cm^3 depending on the diameter of the detector [25-27]. If the impurity concentration is too low, it could result in a high, non-uniform electric field. Conversely, if it is too high, it could result in an excessively high depletion voltage and risk breakdown. Similar issues arise with the dislocation density. Dislocation free crystals do not yield good detectors due to the presence of defects that trap charge carriers, while high dislocation density can lead to problems such as high leakage current, noise, and charge carrier trapping.

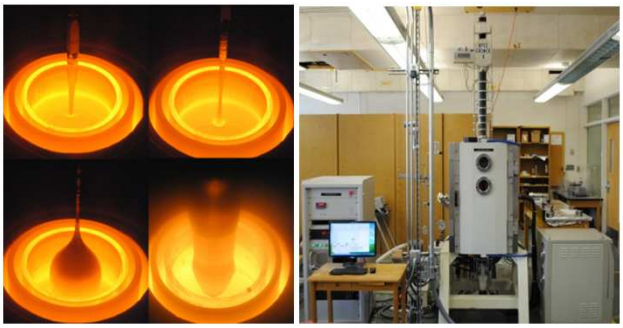

Figure 1. *Crystal growth process (Left) and Crystal grower (Right).*

2.3. Characterization

For the HPGe crystal, the carrier concentration, mobility of charge carrier and resistivity are several important electrical properties that can be used to judge the quality of grown crystals. We use a Vander-Pauw Hall-effect measurement system to measure the electrical properties of grown crystals,

an optical microscope to observe dislocations and calculate density. Using the Vander-Pauw Hall-effect measurement system, both electric field and magnetic fields are applied to the semiconductor. The movement direction of charge carriers are changed due to Lorentz force and Hall electric field, so that the type of crystal (n or p), carrier concentration, electricity and mobility can be determined. For most of zone refinement ingots, we are able to control the carrier concentration at $10^{11}cm^{-3}$, mobility at $4\times10^{4}cm^{2}/V\cdot s$, and the resistivity at $10^{3}\Omega\cdot cm$. For the grown crystal of 10-12cm in diameter, while the mobility and resistivity can be kept at the desirable level, the electronic active impurity levels can be down to $10^{10}cm^{-3}$ to meet the detector-grade requirement [14].

We use Nikon Eclipse LV150L Microscope to observe dislocations and calculate the dislocation density. By measuring and calculating dislocation density, we are able to identify the density and the type of dislocations. These measurements help to determine the best method for crystal growth so that crystal can be grown consistently. The small samples after Hall-effect measurements are polished and etched before optical observations. We measured dislocation densities across the entire cross-section of the grown crystals using the microscope and were able to identify the density and the type of dislocations. We observed that the dislocation density across the large grown crystal may not distribute uniformly, however, there are more dislocations at the edge part of the crystal. The dislocation density existing in grown crystals has been in the range of 10^{2}-$10^{4}/cm^{2}$ (Fig. 2). In addition, photo-thermal ionization spectroscopy (PTIS) was used to identify the impurities in crystals at 7K using a liquid helium cryostat.

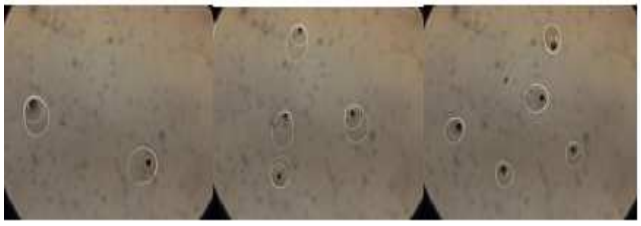

Figure 2. *The dislocations in the top (left), middle (middle) and bottom (right) portions of a Ø12cm <100> crystal (USD No.20). For these images, the area shown is 300x400μm². The dislocation densities are 2000, 3400 and 4200cm⁻² for left, middle and right, respectively.*

2.4. Detector Development

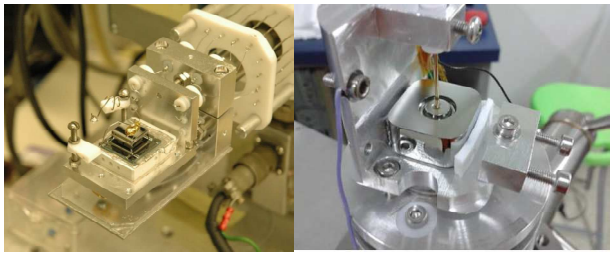

Figure 3. *Detector fabricated by LBNL (Left) and Tsinghua University (Right) using the USD crystals.*

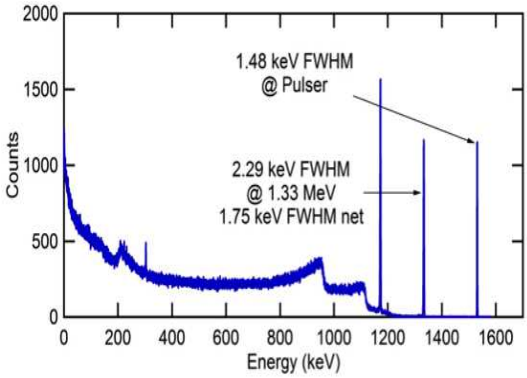

Figure 4. *Energy spectrum of ^{60}Co measured with a HP-Ge detector of the configuration shown in Fig. 3 (Left). The detector was operated with a voltage bias of 3000V, and a pulse peaking time of 8ms was used for the measurement.*

The detector development laboratory includes two clean-rooms: a 300sq. ft. class-100 and a 300sq. ft. class-1000 clean-room. Following an onsite qualification and inspection, the necessary equipment/systems were installed in the detector laboratory. We have collaborated successfully with Mark Amman at LBNL (Fig. 3, Left) and Yulan Li at Tsinghua University (Fig. 3, Right) to fabricate Ge detectors with the crystals from USD, both showed very good energy resolution. Fig. 4 shows an energy spectrum from ^{60}Co taken with the detector made by Mark Amman at LBNL, as an example.

3. Monte Carlo Simulation

3.1. Modeling of Geometry and Material

The geometry of an array of planar detectors was modeled in a Geant4 [32] based Monte Carlo simulation package [33], as shown in Fig. 5. It contains 7 strings. There are 24 copper cans in each string. The wall of a copper can is 0.1cm thick. A string of detectors are mounted in 3 copper rods, fixed on a copper plane at the bottom. Each copper can contain 1 planar detector. Hence, there are 168 planar germanium detectors in total. The diameter and thickness of each detector were chosen to be 10cm and 1cm, respectively, to optimize the time resolution. The mass of each detector is about 0.42kg. The detailed information of the dimensions and materials of the array is summarized in Table 1. Note that the shielding around the detector array was neglected.

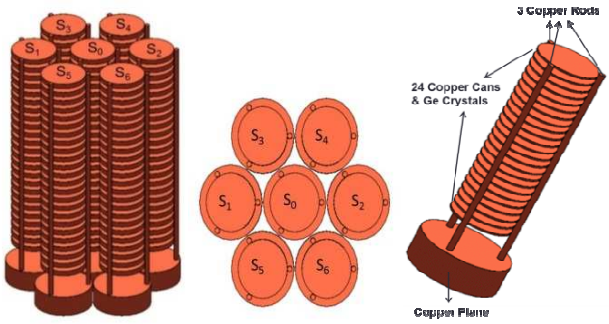

Figure 5. *Schematic of the simulated detector array. Left: Side view. Middle: Top view. Right: The structure of each string. S_i (i=0, 1, 2, 3, 4, 5, 6) represents the string number.*

Table 1. *Dimensions and materials of each crystal (detector), copper can, copper rod and copper plane.*

Components	Diameter (cm)	Height (cm)	Material
Crystal	10.0	1.0	Ge
Copper Can	10.2	0.1	OFHC Copper
Copper Rod	1.0	56.8	OFHC Copper
Copper Plane	13.0	5.0	OFHC Copper

Note that the material of the copper can, copper rod, and copper plane used in the simulation is assumed to be Oxygen-Free High-Conductivity (OFHC) copper, a common shielding material for low-background detectors.

3.2. Simulation Implementation

We simulate the γ-ray background from ^{238}U, ^{232}Th and ^{40}K which are uniformly distributed in all components made of OFHC copper. WIMPs deposit energy only in one detector per interaction, while γ-ray background may deposit energy in several detectors simultaneously. This feature can be used to reject γ-ray background events. The background rejection power was estimated based on this simulation.

The energy threshold of the detectors in the simulation was assumed to be 0.1keV. The analysis was done using events in the energy region of interest (ROI), 0.1 - 10keV.

4. Simulation Results

4.1. Background Rejection Power

The background rejection power of this setup was quantitatively estimated using the granularity reduction factor (GRF) defined as:

$$GRF = \frac{SDEs+MDEs}{SDEs} \quad (1)$$

Where, SDEs (MDEs) denotes the total number of single-detector events (multiple-detector events).

The simulated detector array in Fig. 5 can be treated as 168 independent planar detectors or 7 strings from S_0 to S_6 with 24 detectors in each string or 24 layers with 7 detectors in each layer. It is interesting to study the distributions of the granularity reduction factor among 168 detectors (Fig. 6 – Fig. 8), 24 layers (Fig.9) and 7 strings (Fig. 10) for ^{238}U, ^{232}Th and ^{40}K. The simulation results from Fig. 6 to Fig.8 show that those detectors in the middle of each string has superior background rejection factor since they are surrounded by other detectors and therefore have greater chance for MDEs to occur. Similarly, Fig. 9 and Fig. 10 show the detectors in middle layer and string have greater background rejection power due to their location. Thus, we conclude that the granularity reduction factor has strong position dependence. This agrees with the previous work by Mei. *et al.* [34].

Moreover, the average granularity reduction factors vary with the type of background sources as shown in Table 2. About 19.7%, 22.5% and 31.2% of the events are SDEs in the ROI for ^{238}U, ^{232}Th and ^{40}K, respectively. Hence, most of the background events can be rejected through detector granularity.

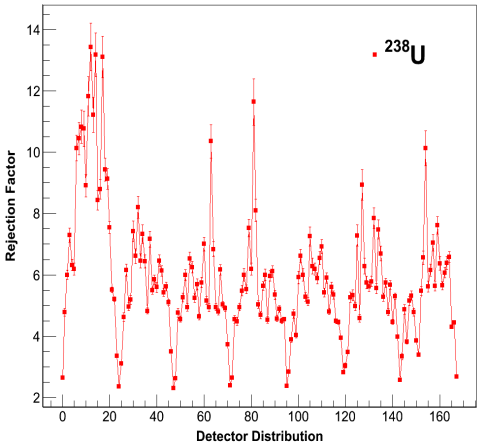

Figure 6. *Granularity reduction factor versus 168 detectors for the events in the ROI for ^{238}U. Detector distribution values 0 - 23 represent the rejection factor for the S_0string from top to bottom. The error bars are statistical errors.*

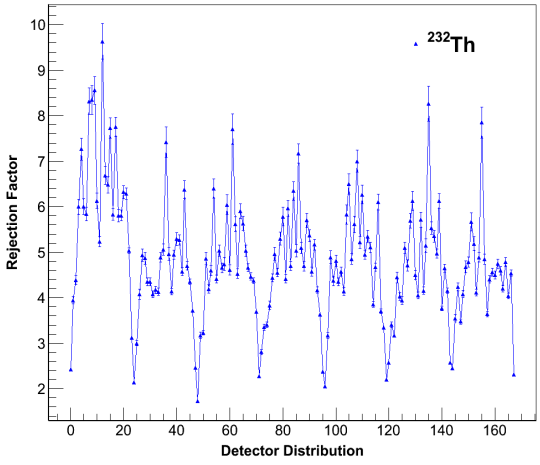

Figure 7. *Granularity reduction factor versus 168 detectors for the events in the ROI for ^{232}Th. Detector distribution values 0 - 23 represent the rejection factor for the S_0 string from top to bottom. The error bars are statistical errors.*

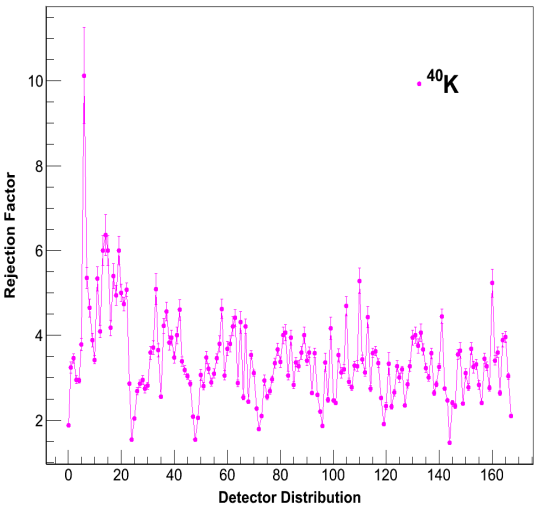

Figure 8. *Granularity reduction factor versus 168 detectors for the events in the ROI for ^{40}K. Detector distribution values 0 - 23 represent the rejection factor for the S_0 string from top to bottom. The error bars are statistical errors.*

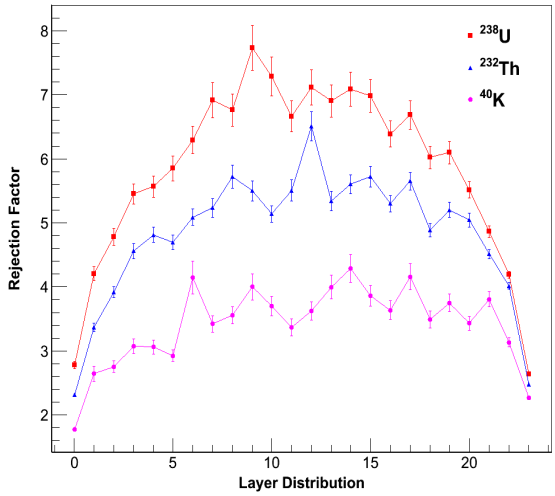

Figure 9. *Granularity reduction factor versus 24 layers for the events in the ROI. The layer distribution values, 0 - 23, correspond to 24 layers from top to bottom for the whole detector array in Fig. 5. The error bars are statistical errors.*

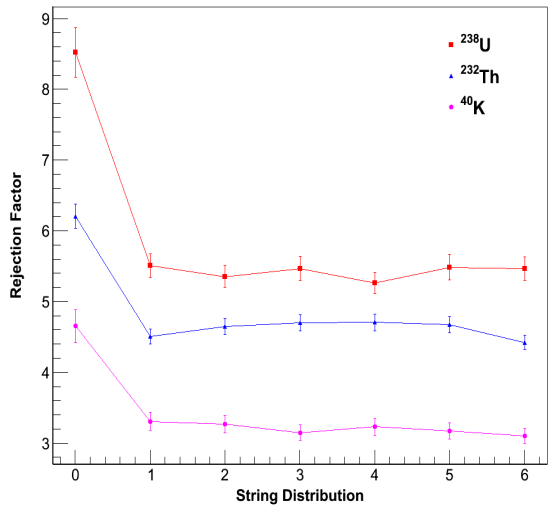

Figure 10. *Granularity reduction factor versus 7 strings for the events in the ROI. String distribution values 0 - 6 represent the rejection factor for 7 strings from S_0 to S_6 as shown in Fig. 5. S_0 has superior rejection factor because it is surrounded by other strings. The error bars are statistical errors.*

Table 2. *Single-detector events (SDEs), multiple-detector events (MDEs) and the average rejection factor of ^{238}U, ^{232}Th and ^{40}K in the ROI. The total decay events for each source are 20 million.*

Background Source	SDEs	MDEs	Granularity Reduction Factor
^{238}U	11422	47194	5.132
^{232}Th	13026	44956	4.451
^{40}K	7341	16264	3.216

In addition to the study of background rejection factor, we also studied the background event rate for ^{238}U, ^{232}Th and ^{40}K. The radioactivity of ^{238}U, ^{232}Th and ^{40}K in the OFHC copper are taken from [35]. As shown in Table 3, the average background rate is about 0.074 events/kg/keV/y based on the percentage of ^{238}U, ^{232}Th and ^{40}K are 35.6%, 41.4% and 23%, respectively. It is worthwhile noticing that the background rate as low as 0.00354 events/kg/keV/y can be achieved if we use the ultra-high purity electroformed copper as the shielding material for this detector array with the radioactivity of ^{238}U, ^{232}Th and ^{40}K provided by [36].

Table 3. *Background event rate of ^{238}U, ^{232}Th and ^{40}K in the ROI.*

Background Source	Radioactivity (μBq/kg)	Background Event Rate (events/kg/keV/y)
^{238}U	16	0.0433
^{232}Th	19	0.0586
^{40}K	88	0.153

4.2. Detector Sensitivity

Our goal in this work is to see whether this new-type of Ge-based planar detector shown in Fig. 5 is able to reach the sensitivity of $\sim 10^{-48} cm^2$, which corresponds to $\sim 2.0\times10^{-5}$ events/70.21kg/y (where 70.21kg is the total mass of the crystals in this simulation), or $\sim 2.9\times10^{-4}$ events/ton/y, assuming that the mass of the WIMP is 100GeV, WIMP mass density is $0.3 GeV/cm^3$ and the velocity of WIMP is 220km/s.

From section 4.1, the background event rate after multi-detector cut is ~0.074 events/kg/keV/y, which is equivalent to ~52 events/70.21kg/y or ~740 events/ton/y in the ROI. In addition, the NR/ER discrimination power of the designed planar germanium detector was examined. It has been observed in silicon detectors that the transportation of charge carriers created by heavily ionizing particles is delayed due to strong electric field inside the ionized plasma zone [37-41]. This is the so-called plasma effect. There are contradicting statements on the plasma effect in germanium in literatures [37, 42]. A preliminary model was built to estimate the time delay of charge transportation for NR events compared to that for ER events. It showed visible difference in the charge transportation time between NR and ER events. If a cut is applied to reject ER events based on the transportation time, the sensitivity in detecting low mass WIMPs as shown in Fig. 11 can be achieved. Note that the energy range (0.57 – 37.08keV) in Fig. 11 is the nuclear recoil energy range that corresponds to the ROI in this work, 0.1 – 10keV, the visible energy.

5. Conclusion

A new type of germanium detector is under development at the University of South Dakota. It features an excellent time resolution below 10ns. This is achievable given: 1) ultra-pure germanium crystals grown locally; and 2) a planar geometry design that shortens the rise time significantly. It has been demonstrated that germanium crystals with an impurity level with $10^{10}/cm^3$ can be grown regularly with the large crystal growth facility at USD. An array of such detectors was modeled in a Geant4-based Monte Carlo simulation package. Based on the simulation, 76.4% of background events from ^{238}U, ^{232}Th and ^{40}K uniformly distributed in detector components can be rejected if it is required that only single detector has energy deposit. A preliminary model was built to estimate the significance of the plasma effect in germanium.

The difference of the charge transportation time between NR and ER events resulted from the plasma effect was used to reject ER events. The sensitivity of detecting WIMP signal after these two criteria applied was ~7.4 $\times 10^{-6}$ events/ton/y in the region of interest (0.1 - 10keV), while the goal of the work was 2.9×10^{-4} events/ton/y corresponding to a spin-independent WIMP-nucleon cross section of ~10^{-48}cm^2. Experiments to verify the plasma effect in germanium detector are planned.

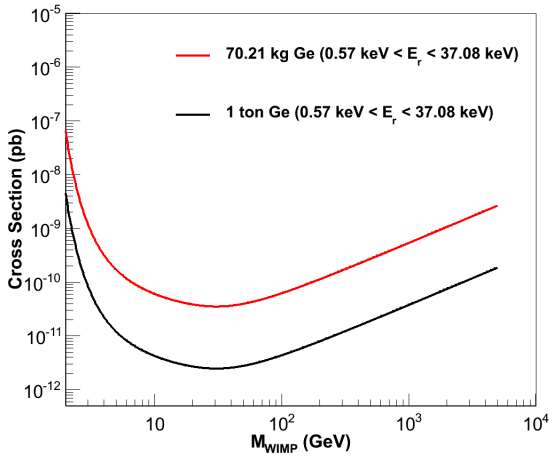

Figure 11. *Anticipated sensitivity for the proposed stringed planar germanium detector with 70.21kg and 1-ton mass. The live time is 1-year.*

Acknowledgements

The authors wish to thank Mark Amman from Lawrence Berkeley National Laboratory and Yulan Li from Tsinghua University in China for fabricating germanium detectors using the USD crystals. This work was supported in part by the NSF PHY-0758120, PHYS-0919278, PHYS-0758120, PHYS-1242640, DOE grant DE-FG02-10ER46709, the Office of Research at The University of South Dakota and a 2010 research center support by the State of South Dakota.

Nomenclature

Germanium (Ge) detector; Dark matter; Weakly Interacting Massive Particles (WIMPs); Nuclear recoils (NR); Electronic recoils (ER); Ge zone refinement; Ge crystal growth; Granularity.

References

[1] K. Kuijken and G. Gilmore, "The mass distribution in the galactic disc - Part III - the Local Volume Mass Density", Monthly Notices of the Royal Astronomical Society 239: 651 (1989).

[2] F. Zwicky, "Die Rotverschiebung von extragalaktischen Nebeln", Helvetica Physica Acta6: 110–127 (1933).

[3] F.Zwicky, "On the Masses of Nebulae and of Clusters of Nebulae", The Astrophysical Journal 86: 217 (1937).

[4] G. Jungman, M. Kamionkowski, and K. Griest, "Supersymmetric dark matter", Physics Reports 267 (1996) 195-373.

[5] R. Bernabei, P. Belli, F. Cappella, R. Cerulli, C.J. Dai, A. d'Angelo, H.L. He, A. Incicchitti, H.H. Kuang, J.M. Ma, F. Montecchia, F. Nozzoli, D. Prosperi, X.D. Sheng, and Z.P. Ye, "First results from DAMA/LIBRA and the combined results with DAMA/NaI", Eur.Phys.J. C56 (2008) 333.

[6] EDELWEISS Collaboration, "Final results of the EDELWEISS-II WIMP search using 4-kg array of cryogenic germanium detectors with interleaved electrods", Phys. Lett. B 702 (2011) 329.

[7] CDMS Collaboration, "Search for Weakly Interacting Massive Particles with teh first five-tower data from the cryogenic dark matter searches at Soudan underground laboratori", Phys. Rev. Lett. 102 (2009) 011301.

[8] ZEPLIN-III Collaboration, "WIMP-nucleon cross-section results from the second science run of ZEPLIN-III", Phys. Lett. B 709 (2012) 14.

[9] XENON100 Collaboration, "Dark matter results from 100 live days of Xenon100 data", Phys. Rev. Lett. 107 (2011) 131302.

[10] CDMS Collaboration, "Results from a low-energy analysis of the CDMS-II germanium data", Phys. Rev. Lett. 106 (2011) 131302.

[11] CoGeNT Collaboration, "Results from a search for light-mass dark matter with a p-type point contact germanium detector", Phys. Rev. Lett. 106 (2011) 131301.

[12] CDMS Collaboration, "Silicon detector dark matter results from the final exposure of CDMS II", Phys. Rev. Lett. 111 (2013) 251301, arXiv:1304.4279.

[13] XENON100 Collaboration, "Dark matter results from 225 live days of XENON100 data", Phys. Rev. Lett. 109 (2012)181301.

[14] D. S. Akerib *et al.* (LUX Collaboration), "First Results from the LUX dark matter experiment at the Sanford underground Research facility", Phys. Rev. Lett. 112, 091303 (2014), arXiv: 1310.8214.

[15] R. Agnese *et al.* (SuperCDMS Collaboration), "Silicon Detector Dark Matter Results from the Final Exposure of CDMS II". arXiv: 1304.4279v3 (2013).

[16] G. Bellini *et al.*, (Borexino Collaboration), "First evidence of pep solar neutrinos by direct detection in Borexion", arXiv:1110.3230.

[17] G. Wang, Y. Sun, G. Yang, W. Xiang, Y. Guan, D. Mei, C. Keller, and Y.-D. Chan, "Development of large size high-purity germanium crystal growth", Journal of Crystal Growth, 352 (1), 27-30 (2012).

[18] G. Yang, G. Wang, W. Xiang, Y. Guan, Y. Sun, D. Mei, B. Gray, and Y.-D. Chan, "Radial and axial impurity distribution in high-purity germanium crystals", Journal of Crystal Growth, 352 (1), 43-46 (2012).

[19] G. Yang, D. Mei, J. Govani, G. Wang, and M. Khizar, "Effect of annealing on contact performance and electrical properties of p-type high purity germanium single crystal", Applied Physics A, DOI 10.1007/s00339-012-7518-x (2013).

[20] G. Wang, Y. Sun, Y. Guan, D. Mei, G. Yang, A. A. Chiller, and B. Gray, "Optical Methods in Orientation of High-Purity Germanium Crystal", Journal of Crystallization Process and Technology, 3, 60-63 (2013).

[21] M. Khizar, G. Yang, G. Wang, W. Xiang, J. Govani, D. Mei, C. Keller, and Y. –D. Chan, "Electrical Characterization of Self-Diffused Li-In/Ga Eutectic, In/Sn Solder and In/Ga Eutectic Ohmic Contacts on n-type <100> Single Crystal HPGe", JP Journal of Structures and Solids, 6, 97-110 (2012).

[22] G. Wang, "CUBED crystal growth", The Workshop on germanium detectors and technology, September 14-17th, Vermillion, SD.

[23] Gang Yang, Jayesh Govani, Hao Mei, Yutong Guan, Guojian Wang, Mianliang Huang, and Dongming Mei, "Investigation of influential factors on the purification of zone-refined germanium ingot", Crystal Research and Technology, March, 2014; DOI: 10.1002/crat.201300418.

[24] Guojian Wang, Mark Amman, Hao Mei, Dongming Mei, Klaus Irmscher, Yutong Guan, and Gang Yang, "Crystal growth and detector performance of large-size HP-Ge crystals", submitted to the Journal of Crystal Growth Technology.

[25] W.L Hansen, Nuclear Instruments and Methods 94 (1971) 377–380.

[26] P. A. Glasow and E. E. Haller, IEEE Transactions on Nuclear Science 23 (1976) 92-96.

[27] E. E. Haller, W. L. Hansen, G. S. Hubbard, F. S. Goulding, Nuclear Science, IEEE Transactions on 23 81-87.

[28] E. E. Haller *et al.*, Nuclear Science, IEEE Transactions on 20 481-487.

[29] W. L. Hansen *et al.*, Nuclear Science, IEEE Transactions on 29 738-744.

[30] W. L. Hansen and E. E. Haller, IEEE Transactions on Nuclear Science 21 (1974) 251- 259.

[31] G. S. Hubbard *et al.*, Nuclear Science, IEEE Transactions on 25 362-370.

[32] S. Agostinelli*et al.*, NIM A 506 (2003) 250-303.

[33] Wenzhao Wei, "Development of a New Type of Germanium Detector for Dark Matter Searches", A Master Thesis at The University of South Dakota.

[34] D.-M. Mei, C. Keller, and Z.-B. Yin, "Increased sensitivity of effective neutrino mass in next generation germanium-based double-beta decay experiment", Internal Research Notes.

[35] Heusser G., M. Laubenstein, and H. Neder, "Low-level germanium gamma-ray spectrometry at the μBq/kg level and future developments towards higher sensitivity".

[36] C. E. Aalseth, The presentation in the DUSEL workshop in Nov. 2-4 of 2007, Washington D.C.

[37] W. Seibt, K. E. Sundstrom, and P. A. Tove, "Charge collection in silicon detectors for strongly ionizing particles", Nuclear Instruments and Methods, 113 (1973) 317-324.

[38] P. A. Tove, W. Seibt, and K. E. Sundstrom, Proc. IspraSymp. Nuclear electronics (6-9 May 1969) p. 101; also UUIP-649 (May 1969).

[39] M. A. Nicolet, J. Appl. Phys. 37 (1966) 4224.

[40] J. B. A. England and G. M. Field, "Z-Identification of charged particles by signal risetime in silicon surface barrier detectors", Nuclear Instruments and Methods in Physics Research A 280 (1989) 291-298.

[41] Z. Sosin, "Description of the plasma delay effect in silicon detectors", arXiv: 1201.2188v1 (2012).

[42] J. Ljungvall and J. Nyberg, "A Study of fast neutron interactions in high-purity germanium detectors", Nuclear Instruments and Methods in Physics Research A 546 (2005) 553-573.